

# Synthesis, Optical Resolution, and X-ray Crystal Structure of a Helical Hexaazamacrocyclic Zinc Complex

L. Henry Bryant, Jr., Abdessadek Lachgar, Kimberly S. Coates, and Susan C. Jackels\*

Department of Chemistry, Wake Forest University, Winston-Salem, North Carolina 27109

Received November 12, 1993\*

The synthesis and structural characterization of the zinc complex of an 18-membered macrocyclic ligand containing four saturated amines and two pyridine groups are described. The compound is formulated as (3,6,14,17,23,24-hexaazatricyclo[17.3.1.1<sup>8,12</sup>]tetracos-1(23),8,10,12(24),19,21-hexaene)zinc(2+) trifluoromethanesulfonate,  $[\text{Zn}(\text{pyo}_2[18]\text{dieneN}_6)](\text{CF}_3\text{SO}_3)_2$ . The proton-NMR spectrum of the complex is consistent with  $D_2$  symmetry in which the ligand is hexacoordinated in a meridional wrap with the pyridine groups twisted relative to each other and the  $-\text{CH}_2\text{NHC}_2\text{H}_4\text{NHCH}_2-$  groups forming helical linkages connecting the pyridine groups. Well defined multiplets in the NMR spectra were analyzed by spin simulation, and the resulting dihedral angles were in agreement with those determined in the solid-state by X-ray crystallography. The complex was inert to both NH and metal ion exchange in aqueous solution. The right- and left-handed helical enantiomers were resolved by formation of diastereomers with (+)-tartrate. The CD spectra gave positive and negative Cotton effects at 262 nm corresponding to the pyridine  $\pi$  to  $\pi^*$  transition.  $[\text{Zn}(\text{pyo}_2[18]\text{dieneN}_6)](\text{CF}_3\text{SO}_3)_2$  ( $\text{ZnC}_{20}\text{N}_6\text{H}_{26}\text{S}_2\text{O}_6\text{F}_6$ ) crystallizes in the orthorhombic space group  $Imcb$  ( $Ibam$ ) with  $Z = 4$ ,  $a = 15.851(4)$  Å,  $b = 18.391(5)$  Å,  $c = 9.325(5)$  Å, and  $V = 2718.4(17)$  Å<sup>3</sup>. X-ray crystallographic results showed that the complex has 222 ( $D_2$ ) symmetry in the solid state, which is the same structure as found in solution.

## Introduction

Zinc complexes of azamacrocycles have been of great interest for their abilities to promote transesterification of RNA,<sup>1</sup> to act as models for hydrolytic enzymes,<sup>2</sup> and to act as mimics of the zinc-base bifunctional catalysis of many enzymes.<sup>3</sup> The polyazacycloalkane complexes with the general formula  $[3k]\text{aneN}_k$  (with  $k = 3-12$ ) have been widely studied.<sup>4-7</sup> For mononuclear complexes of this series, the stability in aqueous solution is greatest for  $[\text{Zn}([15]\text{aneN}_5)]^{2+}$ . This result has been explained by assuming that only five nitrogen donor atoms can be involved in the coordination of the macrocycles to  $\text{Zn}^{2+}$ .<sup>6,7</sup> The lower binding constant for  $[\text{Zn}([18]\text{aneN}_6)]^{2+}$  has been attributed either to the increased flexibility of the ligand<sup>6</sup> or to the sixth unbound donor atom that produces a large strained chelate ring.<sup>6,7</sup>

Multidentate chelates of  $\text{Zn}^{2+}$  having one or more pyridine rings have also been widely studied.<sup>8</sup> Such chelating agents generally bind to metal ions more effectively than the aliphatic amines because pyridine groups have higher dipole moments and lower proton affinities and, when incorporated through 2- or 6-aminomethyl groups, provide chelate rings with lower ring strain.<sup>9</sup> Pyridine has been incorporated into zinc macrocycles in order to influence the flexibility of the macrocycle, to achieve

various coordination numbers for  $\text{Zn}^{2+}$ , and to stabilize unusual coordination geometries.<sup>10-18</sup> Compared to the case of aliphatic azamacrocycles, the rate of complexation of  $\text{Zn}^{2+}$  to analogous pyridine-containing macrocycles is about 10 times slower.<sup>19</sup> Presumably, this decrease in rate is due to the lower flexibility of the macrocycle or to steric effects. Synthetic schemes for these macrocyclic complexes either have used  $\text{Zn}^{2+}$  as a templating metal ion<sup>10,14,16,17,20</sup> or have complexed zinc to the preformed metal-free macrocycle.<sup>12,14,15,18,21,22</sup> The coordination geometries and possible isomeric forms of the zinc macrocyclic complexes have been analyzed by NMR and X-ray crystallography.<sup>14,15,17,18,21-23</sup>

Rothermel et al.<sup>24</sup> have reported the synthesis of the 18-membered hexaazamacrocyclic containing two pyridine groups and four aliphatic amines  $\text{pyo}_2[18]\text{dieneN}_6$ , shown in Figure 1. The zinc complex of this macrocycle has stability ( $\log K^{\text{ML}} = 21.1$ ) greater than those of the analogous  $[18]\text{aneN}_6$  and  $[15]\text{aneN}_5$  complexes, suggesting that the macrocycle coordinates through all six nitrogen atoms. Due to the four asymmetric

\* Abstract published in *Advance ACS Abstracts*, March 15, 1994.

- (1) Shelton, V. M.; Morrow, J. R. *Inorg. Chem.* **1991**, *30*, 4295-4299.
- (2) (a) Bertini, I.; Luchinat, C.; Maret, W.; Zeppezauer, M. *Zinc Enzymes*; Birkhäuser: Boston, MA, 1988. (b) Vallee, B. L.; Galdes, A. *Advances in Enzymology*; Wiley: New York, 1984; Vol. 56, p 283. (c) Koike, T.; Kimura, E.; Nakamura, I.; Hashimoto, Y.; Shiro, M. *J. Am. Chem. Soc.* **1992**, *114*, 7338-7345. (d) Kimura, E.; Shioita, T.; Koike, T.; Shiro, M.; Kodama, M. *J. Am. Chem. Soc.* **1990**, *112*, 5805-5811.
- (3) Breslow, R.; Berger, D.; Huang, D. *J. Am. Chem. Soc.* **1990**, *112*, 3686-3687.
- (4) Kodama, M.; Kimura, E. *J. Chem. Soc., Dalton Trans.* **1977**, 2269-2276.
- (5) Kodama, M.; Kimura, E. *J. Chem. Soc., Dalton Trans.* **1978**, 1081-1085.
- (6) Kodama, M.; Kimura, E.; Yamaguchi, S. *J. Chem. Soc., Dalton Trans.* **1980**, 2536-2538.
- (7) Beneini, A.; Bianchi, A.; Dapporto, P.; Garcia-España, E.; Micheloni, M.; Paoletti, P. *Inorg. Chem.* **1989**, *28*, 1188-1191.
- (8) Newkome, G. R.; Strekowski, L., Eds. *Pyridine-Metal Complexes*; Wiley: New York, 1985; Vol. 14, Part 6A.
- (9) Timmons, J. H.; Martell, A. E.; Harris, W. R.; Murase, I. *Inorg. Chem.* **1982**, *21*, 1525-1529.

- (10) Alcock, N. W.; Liles, D. C.; McPartlin, M.; Tasker, P. A. *J. Chem. Soc., Chem. Commun.* **1974**, 727-728.
- (11) Dabrowiak, J. C.; Nafie, L. A.; Bryan, P. S.; Torkelson, A. T. *Inorg. Chem.* **1974**, *16*, 540-544.
- (12) Drew, M. G. B.; Hollis, S. *J. Chem. Soc., Dalton Trans.* **1978**, 511-516.
- (13) Lindoy, L. F.; Busch, D. H. *Inorg. Chem.* **1974**, *13*, 2494-2498.
- (14) Radecka-Paryzek, W. *Inorg. Chim. Acta* **1979**, *34*, 5-8.
- (15) Adam, K. R.; Donnelly, S.; Leong, A. J.; Lindoy, L. F.; McCool, B. J.; Bashall, A.; Dent, M. R.; Murphy, B. P.; McPartlin, M.; Fenton, D. E.; Tasker, P. A. *J. Chem. Soc., Dalton Trans.* **1990**, 1635-1643.
- (16) Liles, D. C.; McPartlin, M.; Tasker, P. A. *J. Chem. Soc., Dalton Trans.* **1987**, 1631-1636.
- (17) Haque, Z. P.; McPartlin, M.; Tasker, P. A. *Inorg. Chem.* **1979**, *18*, 2920-2921.
- (18) Alcock, N. W.; Moore, P.; Omar, H. A. A.; Reader, C. J. *J. Chem. Soc., Dalton Trans.* **1987**, 2643-2648.
- (19) Schultz-Grunow, P.; Kaden, T. A. *Helv. Chim. Acta* **1978**, *61*, 2291-2296.
- (20) Prince, R. H.; Stotter, D. A.; Woolley, P. R. *Inorg. Chim. Acta* **1974**, *9*, 51-54.
- (21) Lewis, J.; O'Donoghue, T. *J. Chem. Soc., Dalton Trans.* **1980**, 743-749.
- (22) Alcock, N. W.; Balakrishnan, K. P.; Berry, A.; Moore, P.; Reader, C. *J. Chem. Soc., Dalton Trans.* **1988**, 1089-1093 and references therein.
- (23) Lewis, J.; O'Donoghue, T. *Inorg. Chim. Acta* **1978**, *30*, L339-L340.
- (24) Rothermel, G. L., Jr.; Miao, L.; Hill, A. L.; Jackels, S. C. *Inorg. Chem.* **1992**, *31*, 4854-4859.

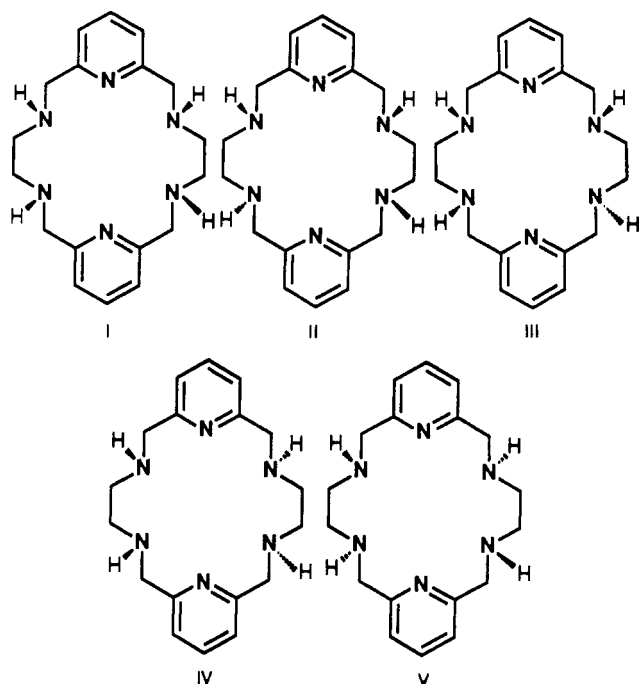


Figure 1. Five possible isomeric forms of  $\text{pyo}_2[18]\text{dieneN}_6$ .

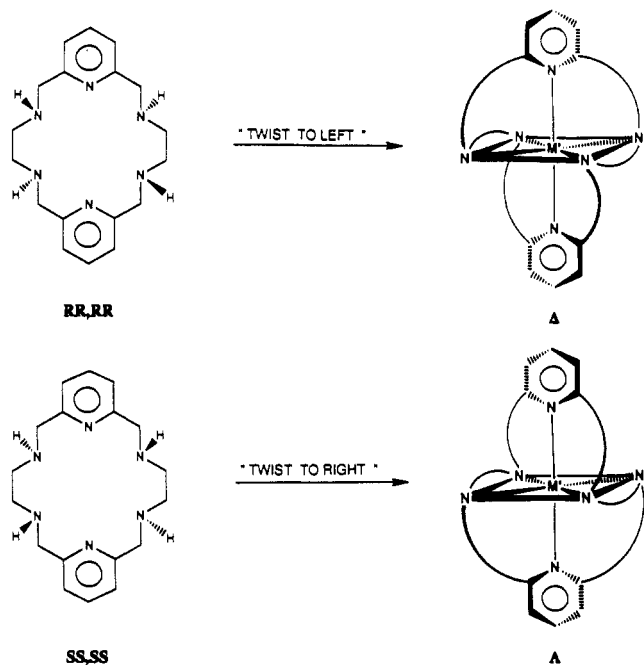


Figure 2. Enantiomeric relationships for  $[\text{Zn}(\text{pyo}_2[18]\text{dieneN}_6)]^{2+}$ .

nitrogen atoms, there are five possible isomers for  $\text{pyo}_2[18]\text{dieneN}_6$  (Figure 1). In order to coordinate through its six nitrogen atoms,  $\text{pyo}_2[18]\text{dieneN}_6$  must twist, pucker, or fold. Whereas  $[18]\text{aneN}_6$  is potentially capable of an octahedral wrap in two modes, corresponding to meridional or facial disposition of nitrogen donors,<sup>25</sup>  $\text{pyo}_2[18]\text{dieneN}_6$  can wrap only in the meridional mode due to the planarity and rigidity imposed by the pyridine groups. An inspection of space-filling models indicates that only isomer V allows  $\text{pyo}_2[18]\text{dieneN}_6$  to twist, forming a pseudooctahedral wrap. Furthermore, each of the enantiomeric forms of isomer V can twist in only one direction, as shown in Figure 2. The direction of the meridional twist in turn produces two enantiomerically related coordinated structures. Thus, in order to interconvert the resulting  $\Delta$  and  $\Lambda$  complexes, both dissociation

and ligand isomerization are necessary. These observations lead to the hypothesis that the complexes of  $\text{pyo}_2[18]\text{dieneN}_6$  could be exceptionally inert even with normally labile metal ions like  $\text{Zn}^{2+}$ .

In this paper, we report the synthesis, characterization, and X-ray crystal structure of  $[\text{Zn}(\text{pyo}_2[18]\text{dieneN}_6)]^{2+}$ . The structure of the complex in solution was determined by NMR and will be compared to the solid-state structure. The optical resolution of the complex is reported. This, to our knowledge, is the first example of a helical macrocyclic zinc complex and its optical resolution.

## Experimental Section

**Preparations.** Barium chloride dihydrate, sodium borohydride, zinc triflate, potassium triflate, and triethylamine were obtained from Aldrich Chemical Co. D-Tartaric acid was obtained from J. T. Baker Chemical Co. Trifluoromethanesulfonic acid was obtained from Eastman Fine Chemicals Laboratory & Research Products. Zinc sulfate, sodium hydroxide, anhydrous methanol, and anhydrous ethyl ether were obtained from Fisher Scientific Co. 2,6-Pyridinedicarbaldehyde was prepared according to a published method.<sup>24,26</sup> All commercial materials were used without further purification.

**3,6,14,17,23,24-Hexaazatricyclo[17.3.1.1<sup>8,12</sup>]tetracos-1(23),8,10,12-(24),19,21-hexaene-Tetrakis(trifluoromethanesulfonic acid) ( $\text{pyo}_2[18]\text{dieneN}_6 \cdot 4\text{CF}_3\text{SO}_3\text{H}$ ).** This ligand was prepared by a modification of the method of Rothermel et al.<sup>24</sup> A solution of ethylenediamine (2.00 mL, 30 mmol) in 20 mL of anhydrous methanol was added dropwise over 15 min to a stirred solution of 2,6 pyridinedicarbaldehyde (4.05 g, 30 mmol) and  $\text{BaCl}_2 \cdot 2\text{H}_2\text{O}$  (3.66 g, 15 mmol) in 150 mL of anhydrous methanol. The mixture was refluxed for 4 h. After the yellow solution was allowed to cool to room temperature,  $\text{NaBH}_4$  (3.0 g, 80 mmol) was added in small portions, the flask was placed in an ice bath, and the mixture was stirred for 30 min. A second addition of  $\text{NaBH}_4$  (1.5 g, 40 mmol) was made in small portions, and the resulting yellow-white mixture was stirred at room temperature for 1.5 h. Evaporation of the solvent under reduced pressure yielded a pale yellow solid. This was extracted with  $4 \times 100$  mL of chloroform, and the extracts were filtered. Evaporation of the combined extracts to dryness under reduced pressure yielded an orange oil. The oil was dissolved in 80 mL of methanol, and trifluoromethanesulfonic acid (10.0 mL, 120 mmol) was added. During the addition, a white solid precipitated (11.4 g, 41% yield; crude tetraprotonated macrocycle). The product was recrystallized by dissolving in a minimum amount of hot methanol to which was added activated carbon. After the mixture was filtered, anhydrous ethyl ether was added to incipient cloudiness while the stirring was maintained. The solution was cooled to room temperature and placed in a refrigerator overnight. The white crystalline solid (61% recovery) was washed with ice-cold anhydrous ethyl ether and stored in a vacuum desiccator. Mp = 192 °C dec. <sup>1</sup>H NMR (DMSO/TMS (ppm)):  $\delta$  = 3.27 (s, 8H), 4.60 (s, 8H), 7.60 (d,  $J$  = 7.8 Hz, 4H), 8.80 (t,  $J$  = 7.8 Hz, 2H), 9.10 (br, 8H). <sup>13</sup>C{<sup>1</sup>H} NMR (DMSO/TMS (ppm)):  $\delta$  = 42.3, 50.0, 123.5, 139.4, 150.7. IR (KBr pellet ( $\text{cm}^{-1}$ )):  $\nu_{\text{C-H}}$  3051–3028 (s), 2968–2947 (m);  $\nu_{\text{N-H}}$  2891–2675 (m);  $\nu_{\text{C=C=N}}$  1599, 1579, 1520, 1469, 1437 (m);  $\nu_{\text{S=O}}$  1303, 1261, 1026 (s);  $\nu_{\text{C-F}}$  1182, 1153 (m);  $\delta_{\text{S=O}}$  632 (s). Anal. Calcd for  $\text{C}_{22}\text{H}_{32}\text{N}_6\text{F}_{12}\text{S}_3\text{O}_{12}$ : C, 28.51; H, 3.26; N, 9.06. Found: C, 28.21; H, 3.48; N, 8.77.

**(3,6,14,17,23,24-Hexaazatricyclo[17.3.1.1<sup>8,12</sup>]tetracos-1(23),8,10,12-(24),19,21-hexaene)zinc(2+) Trifluoromethanesulfonate  $[\text{Zn}(\text{pyo}_2[18]\text{dieneN}_6)](\text{CF}_3\text{SO}_3)_2$ .**  $\text{Zn}(\text{CF}_3\text{SO}_3)_2$  (0.39 g, 1.1 mmol) was added to a methanolic solution of  $\text{pyo}_2[18]\text{dieneN}_6 \cdot 4\text{CF}_3\text{SO}_3\text{H}$  (1.0 g, 1.1 mmol). The pH of the solution was adjusted to neutrality (determined by pH paper) with triethylamine. After the addition, a white solid precipitated. The crude product was dissolved in 20 mL of boiling methanol. After filtration and cooling of the solution to room temperature, colorless crystals formed. The crystals were isolated and dried under vacuum. Yield: 0.49 g (66%). Mp = 264 °C dec. <sup>1</sup>H NMR (DMSO/TMS (ppm)):  $\delta$  = 2.10 (m, 4H), 2.75 (m, 4H), 3.91 (d,  $J$  = 16.8 Hz, 4H), 4.33 (d of d,  $J$  = 5.8 Hz, 4H), 4.55 (br, 4H), 7.54 (d,  $J$  = 7.8 Hz, 4H), 8.11 (t,  $J$  = 7.8 Hz, 2H). <sup>13</sup>C{<sup>1</sup>H} NMR (DMSO/TMS (ppm)):  $\delta$  = 47.5, 49.7, 122.2, 141.1, 154.5. IR (KBr pellet ( $\text{cm}^{-1}$ )):  $\nu_{\text{N-H}}$  3275 (s);  $\nu_{\text{C-H}}$  3094, 3024 (w), 2924, 2883 (m);  $\nu_{\text{C=C=N}}$  1612, 1589, 1462, 1442 (m);  $\nu_{\text{S=O}}$

(25) Searle, G. H. *Bull. Chem. Soc. Jpn.* 1989, 62, 4021–4032.

(26) Papadopoulos, E. P.; Jarrar, A.; Issidorides, C. H. *J. Org. Chem.* 1966, 31, 615–616.

Table 1.  $^{13}\text{C}$ -NMR Spectral Data (DMSO- $d_6$ ;  $\delta$ , ppm)<sup>a</sup>

pyo <sub>2</sub> [18]dieneN <sub>6</sub> ·4CF <sub>3</sub> SO <sub>3</sub> H	[Zn(py <sub>2</sub> [18]dieneN <sub>6</sub> )](CF <sub>3</sub> SO <sub>3</sub> ) <sub>2</sub>	assignment <sup>b</sup>
150.9	154.5	pyridine $\alpha$ -carbon
139.6	141.2	pyridine $\gamma$ -carbon
123.8	122.3	pyridine $\beta$ -carbon
50.2	49.7	methylene carbon adjacent to pyridine
42.3	47.5	carbon of the ethylenic linkage

<sup>a</sup> Chemical shifts relative to internal *p*-dioxane at 66.5 ppm. <sup>b</sup> Assignments based on heteronuclear correlation spectroscopy.

Table 2.  $^1\text{H}$ -NMR Spectral Data (DMSO- $d_6$ ;  $\delta$ , ppm)<sup>a</sup>

pyo <sub>2</sub> [18]dieneN <sub>6</sub> ·4CF <sub>3</sub> SO <sub>3</sub> H	[Zn(py <sub>2</sub> [18]dieneN <sub>6</sub> )](CF <sub>3</sub> SO <sub>3</sub> ) <sub>2</sub>	assignment <sup>b</sup>
9.01 s, 4 H		CF <sub>3</sub> SO <sub>3</sub> H
8.08 t, $J = 7.8$ Hz, 2 H	8.11 t, $J = 7.8$ Hz, 2 H	H <sub>A</sub>
7.60 d, $J = 7.8$ Hz, 4 H	7.54 d, $J = 7.8$ Hz, 4 H	H <sub>B</sub>
	4.56 s, 4 H	H <sub>E</sub>
4.60 s, 8 H	4.33 d of d, $J = 5.8$ Hz, 4 H	H <sub>C</sub>
	3.91 d, $J = 16.8$ Hz, 4 H	H <sub>D</sub>
3.25 s, 8 H	2.75 mult, 4 H	H <sub>F</sub>
	2.10 mult, 4 H	H <sub>G</sub>

<sup>a</sup> Chemical shifts relative to internal TMS at 0.00 ppm. <sup>b</sup> Assignments based on heteronuclear correlation spectroscopy. See Figure 3 for labels.

1296, 1244, 1222, 1024(s);  $\nu_{\text{C-F}}$  1165 (s);  $\delta_{\text{S-O}}$  638 (s). Molar conductivity ( $10^{-3}$  M, aqueous):  $205 \text{ cm}^2 \Omega^{-1} \text{ mol}^{-1}$ . Anal. Calcd for ZnC<sub>20</sub>H<sub>26</sub>N<sub>6</sub>F<sub>6</sub>O<sub>6</sub>S<sub>2</sub>: Zn, 9.47; C, 34.81; H, 3.80; N, 12.18. Found: Zn, 9.79; C, 34.97; H, 3.85; N, 12.20.

**3,6,14,17,23,24-Hexaazatricyclo[17.3.1.1<sup>8,12</sup>]tetracosane-1(23),8,10,12-(24),19,21-hexaene Monohydrate (pyo<sub>2</sub>[18]dieneN<sub>6</sub>·H<sub>2</sub>O).** To pyo<sub>2</sub>[18]dieneN<sub>6</sub>·4CF<sub>3</sub>SO<sub>3</sub>H (15.0 g, 16 mmol) dissolved in 100 mL water was added NaOH (2.59 g, 65 mmol). After 15 min of stirring, a white solid precipitated. The product was recrystallized by dissolving in a minimum amount of hot water. After filtration and cooling of the solution to room temperature, colorless crystals were isolated and dried under vacuum. Yield: 4.7 g (87%). Mp = 158 °C dec.  $^1\text{H}$  NMR (DMSO/TMS (ppm)):  $\delta = 2.60$  (s, 8H), 3.37 (s, 4H), 3.68 (s, 8H), 7.17 (d,  $J = 7.8$  Hz, 4H), 7.65 (t,  $J = 7.8$  Hz, 2H).  $^{13}\text{C}\{^1\text{H}\}$  NMR (DMSO/TMS (ppm)):  $\delta = 49.0, 54.6, 120.6, 136.5, 159.0$ . IR (KBr pellet ( $\text{cm}^{-1}$ )):  $\nu_{\text{O-H}}$  3442 (m);  $\nu_{\text{C-H}}$  3004, 2949 (s);  $\nu_{\text{N-H}}$  3269 (w);  $\nu_{\text{C-C-N}}$  1589, 1575, 1467, 1434 (s). Anal. Calcd for C<sub>18</sub>N<sub>6</sub>H<sub>28</sub>O: C, 62.76; H, 8.19; N, 24.39. Found: C, 62.79; H, 7.82; N, 24.39.

**Optical Resolution of (+)<sub>262</sub>- and (-)<sub>262</sub>-[Zn(py<sub>2</sub>[18]dieneN<sub>6</sub>)](CF<sub>3</sub>SO<sub>3</sub>)<sub>2</sub>.** Zn(SO<sub>4</sub>)·7H<sub>2</sub>O (3.53 g, 12 mmol) was added to an aqueous suspension of pyo<sub>2</sub>[18]dieneN<sub>6</sub> (4.02 g, 12 mmol). Barium (+)-tartrate (3.51 g, 12 mmol) was added, and the suspension was heated for 4 h. The suspension was filtered while hot. Complete removal of SO<sub>4</sub><sup>2-</sup> as BaSO<sub>4</sub> was confirmed by the addition of barium (+)-tartrate to an aliquot of the filtrate. Cooling the solution to room temperature resulted in the formation of colorless crystals of (+)-[Zn(py<sub>2</sub>[18]dieneN<sub>6</sub>)]-(+)-tartrate. The crystals were isolated and dried under vacuum. The other diastereomer was obtained by reducing the volume of solvent under reduced pressure and placing the solution in a refrigerator overnight. A white solid precipitated and was collected by suction filtration. The resulting white solid was dried under vacuum.

To (+)-[Zn(py<sub>2</sub>[18]dieneN<sub>6</sub>)]-(+)-tartrate (0.68 g, 1.26 mmol) dissolved in methanol (50 mL) was added CF<sub>3</sub>SO<sub>3</sub>K (0.47 g, 2.52 mmol). To (-)-[Zn(py<sub>2</sub>[18]dieneN<sub>6</sub>)]-(+)-tartrate (1.99 g, 3.69 mmol) dissolved in methanol (50 mL) was added CF<sub>3</sub>SO<sub>3</sub>K (1.39 g, 7.38 mmol). Both of the resulting methanolic suspensions were filtered to remove potassium (+)-tartrate, and the filtrates were individually evaporated under reduced pressure to obtain (+)<sub>262</sub>-[Zn(py<sub>2</sub>[18]dieneN<sub>6</sub>)](CF<sub>3</sub>SO<sub>3</sub>)<sub>2</sub> (0.66 g;  $\Delta\epsilon_{262} = +12 \pm 1$  mdeg for a 0.1% aqueous solution) and (-)<sub>262</sub>-[Zn(py<sub>2</sub>[18]dieneN<sub>6</sub>)](CF<sub>3</sub>SO<sub>3</sub>)<sub>2</sub> (0.91 g;  $\Delta\epsilon_{262} = -22 \pm 1$  mdeg for a 0.1% aqueous solution). Racemic [Zn(py<sub>2</sub>[18]dieneN<sub>6</sub>)](CF<sub>3</sub>SO<sub>3</sub>)<sub>2</sub> gave  $\Delta\epsilon_{262} = -7 \pm 1$  mdeg for a 0.1% aqueous solution. Thus, applying a 7 mdeg correction for the reading on the racemic mixture gave +19 and -15 mdeg rotations for the 0.1% solutions of the enantiomers, respectively.

**Characterization Methods.** Elemental analyses were carried out by Galbraith Laboratories, Inc., Knoxville, TN. IR spectra were obtained on a Mattson 4020 FT-IR spectrophotometer using KBr pellets. Molar conductance measurements were obtained with a YSI Model 35 conductance meter and an immersion type electrode.  $^1\text{H}$ - and  $^{13}\text{C}$ -NMR spectra were obtained on a Varian VXR-200 spectrometer. The UV spectrum was obtained using a Hewlett Packard 8452A diode array spectrophotometer controlled with HP 89531A software on a Zenith

386/SX computer. Optical rotations were measured at 589 nm in aqueous solution using a 1-dm cell in a Jasco DIP-370 digital polarimeter (*D*-tartrate,  $c = 20$  in H<sub>2</sub>O,  $[\alpha]_{589} = 12.604 \pm 0.002^\circ$ ; lit.<sup>27</sup>  $[\alpha]_{589} = 12.0^\circ$ ). Final reported rotations were an average of 15 scans over a period of 60 s/scan. The circular dichroism spectra were obtained using a Jasco J-720 spectropolarimeter. Calibration of the instrument was checked by comparing the  $\Delta\epsilon_{290.5}$  value for ammonium camphorsulfonate-*d*<sub>10</sub> to the literature value<sup>27</sup> ( $\Delta\epsilon_{290.5} = 190.4$  mdeg).

**[Zn(py<sub>2</sub>[18]dieneN<sub>6</sub>)](CF<sub>3</sub>SO<sub>3</sub>)<sub>2</sub> Crystal Structure.** Investigation of the oscillation and Weissenberg photographs of a crystal mounted on a glass fiber allowed the determination of Laue symmetry *mmm* (orthorhombic) and approximate unit cell parameters. Systematic absences were found to be consistent with two possible space groups: *Imcb* (centrosymmetric) and *I2cb* (noncentrosymmetric). A colorless 0.15 × 0.20 × 0.30 mm<sup>3</sup> crystal suitable for single-crystal X-ray diffraction was found. Data were collected at -100 °C on a Rigaku AFC6S diffractometer using Mo K $\alpha$  radiation,  $\lambda = 0.70930 \text{ \AA}$ , and a graphite monochromator. Accurate unit cell parameters were obtained by least-squares refinement of the setting angles of 25 reflections in the range  $26.34^\circ < 2\theta < 32.45^\circ$ . Intensity data were collected using the  $\omega$ - $2\theta$  scan method up to  $2\theta = 55^\circ$ . Three intensity control reflections were monitored every 200 reflections, resulting in no evidence of crystal deterioration or loss of alignment throughout data collection. A total of 1621 reflections were collected ( $h = 0-20, k = 0-23, l = 0-12$ ); 1021 of the unique reflections had  $I \geq 2.5\sigma(I)$  and were included in the refinement. No absorption correction was applied due to the small magnitude of the absorption coefficient ( $\mu = 11.6 \text{ cm}^{-1}$ ). Table 3 summarizes the most important crystallographic data. The structure was solved using the direct methods program SOLVER of the NRCVAX package.<sup>28</sup> Subsequent least-squares refinement and difference Fourier maps yielded the positions of all the atoms in the asymmetric unit. The atomic position of the hydrogen atom attached to the amine nitrogen atom of the macrocycle was located on a difference electron density map. The remaining hydrogen atom positions were calculated. The triflate counterion exhibited rotational disorder that was modeled. The triflate group was found to be statistically distributed among two independent crystallographic sites with an average refined occupancy of 50%. Final least-squares refinement with hydrogen atoms contributing to the structure factors, and anisotropic thermal parameters for all non-hydrogen atoms converged in three cycles to  $R = 0.052, R_w = 0.059$ , and  $\text{GoF} = 1.80$ . The maximum shift/ $\sigma$  ratio for all the 137 refined parameters was less than 0.02. A final difference Fourier map was featureless, with the deepest hole  $-0.86 \text{ e/\AA}^3$  and the highest residual of  $0.64 \text{ e/\AA}^3$ . Final atomic coordinates and their calculated standard deviations and the calculated positions for the hydrogen atoms are given in Table 6. Tables 4 and 5 give selected bond distances, bond angles, and torsion angles. Complete tables are given in the supplementary material.

(27) Windholz, M. *The Merck Index*; Merck & Co., Inc.: Rahway, N. J., 1983; p 8933.

(28) Gabe, E. J.; LePage, Y.; Eharland, J.-P.; Lee, F. L.; White, P. S. *J. Appl. Crystallogr.* **1989**, *22*, 384-387.

**Table 3.** Summary of Crystallographic Data for [Zn(py<sub>o</sub>2[18]dieneN<sub>6</sub>)](CF<sub>3</sub>SO<sub>3</sub>)<sub>2</sub>

formula	ZnC <sub>20</sub> N <sub>6</sub> H <sub>26</sub> S <sub>2</sub> O <sub>6</sub> F <sub>6</sub>
fw	689.95
crystal system	orthorhombic
space group	<i>Imcb</i> (standard setting <i>Ibam</i> ) <sup>a</sup>
Z	4
a (Å)	15.851(4)
b (Å)	18.391(5)
c (Å)	9.325(5)
V (Å <sup>3</sup> )	2718.4(17)
D <sub>calc</sub> (g cm <sup>-3</sup> )	1.686
D <sub>meas</sub> (g cm <sup>-3</sup> )	1.62
crystal dimensions (mm <sup>3</sup> )	0.15 × 0.20 × 0.30
temperature (°C)	-100
radiation	Mo Kα
scan type	2θ-ω
octants collected	<i>hkl</i>
no. of reflections collected	1621
no. of unique reflections with I ≥ 2.5σ(I)	1021
absorption coefficient (cm <sup>-1</sup> )	11.6
no. of refined parameters	137
R	0.052
R <sub>w</sub>	0.059
goodness of fit	1.80

<sup>a</sup> In the standard space group, the unit cell parameters are *a* = 9.325(5), *b* = 18.391(5), and *c* = 15.851(4) Å.

**Table 4.** Selected Bond Distances (Å) and Angles (deg) in [Zn(py<sub>o</sub>2[18]dieneN<sub>6</sub>)](CF<sub>3</sub>SO<sub>3</sub>)<sub>2</sub><sup>a</sup>

(a) Zinc Environment			
Zn-N1	2.112(5)	Zn-N2	2.210(4)
N1-Zn-N2	75.09(10)	N2-Zn-N2c	82.49(14)
N1-Zn-N2a	104.91(10)	Zn-N1-C3	119.7(3)
N2-Zn-N2a	150.25(13)	Zn-N2-C4	109.2(3)
N2-Zn-N2b	150.18(14)	Zn-N2-C5	103.99(25)
(b) Ligand (C <sub>18</sub> H <sub>22</sub> N <sub>6</sub> )			
N1-C3	1.328(5)	C2-C3	1.381(7)
N2-C4	1.467(6)	C3-C4	1.503(8)
N2-C5	1.477(6)	C5-C5c	1.509(9)
C1-C2	1.375(9)		
C3-N1-C3b	120.6(5)	N1-C3-C4	114.2(4)
C4-N2-C5	111.7(3)	C2-C3-C4	124.6(5)
C2-C1-C2b	119.8(6)	N2-C4-C3	110.5(4)
C1-C2-C3	118.6(6)	N2-C5-C5c	110.0(4)
N1-C3-C2	121.2(5)		

<sup>a</sup> Atoms X and Xa are symmetry related by the 2-fold axis in Figure 7 that includes Zn and is perpendicular to the plane of the page (see Figure 7). Atoms X and Xb are related by the 2-fold axis passing through C1, N1, and Zn. Atoms X and Xc are related by the 2-fold axis bisecting the carbon-carbon bonds of the ethylenic linkages.

**Table 5.** Selected Torsion Angles (deg) for [Zn(py<sub>o</sub>2[18]dieneN<sub>6</sub>)](CF<sub>3</sub>SO<sub>3</sub>)<sub>2</sub><sup>a</sup>

Zn-N2-C4-C3	36.5(2)	HN2-N2-C5-H5b	171.1(7)
Zn-N2-C4-H4b	-85.2(4)	HN2-N2-C5-H5	53.0(3)
Zn-N2-C5-H5b	-75.6(3)	HN2-N2-C4-C3	153.5(6)
N1-Zn-N2-C5	92.4(3)	C4-N2-C5-H5b	42.0(3)
N2-Zn-N1-C3	13.8(2)	C4-N2-C5-H5a	-76.0(4)
HN2-N2-C4-H4b	31.8(2)	C5-N2-C4-H4a	160.4(6)
HN2-N2-C4-H4a	-84.8(5)	C5-N2-C4-H4b	43.8(3)

<sup>a</sup> Atom numbers refer to Table 6.

## Results and Discussion

**Synthesis.** The macrocyclic ligand salt py<sub>o</sub>2[18]dieneN<sub>6</sub>·4CF<sub>3</sub>SO<sub>3</sub>H was prepared by barium template condensation of ethylenediamine and 2,6-pyridinedicarbaldehyde followed by reduction based on a previous methodology.<sup>24</sup> The tetraprotonated ligand was obtained metal-free and analytically pure in 41% yield as the triflate salt. The NMR and IR spectra, elemental analyses, and potentiometric titration of H<sup>+</sup> equivalents all are consistent

**Table 6.** Atomic Parameters *x*, *y*, *z* in Fractions of the Unit Cell Dimensions and Isotropic Thermal Parameters for [Zn(py<sub>o</sub>2[18]dieneN<sub>6</sub>)](CF<sub>3</sub>SO<sub>3</sub>)<sub>2</sub><sup>a</sup>

atom	<i>x</i>	<i>y</i>	<i>z</i>	B <sub>iso</sub> (Å <sup>2</sup> )
Zn	1/4	0	1/2	1.96(4)
N1	1/4	0.11484(24)	1/2	2.87(22)
N2	0.16537(22)	0.03092(21)	0.3218(4)	2.75(14)
C1	1/4	0.2632(4)	1/2	8.3(7)
C2	0.1908(4)	0.2257(3)	0.4216(7)	5.9(3)
C3	0.1921(3)	0.1506(3)	0.4251(6)	3.52(20)
C4	0.1286(3)	0.1025(3)	0.3519(5)	3.95(22)
C5	0.2214(3)	0.0328(3)	0.1953(5)	2.91(17)
HN2	0.124	-0.007	0.317	3.5
H1	1/4	0.315	1/2	9.1
H2	0.149	0.250	0.365	6.7
H4a	0.110	0.124	0.264	4.7
H4b	0.079	0.097	0.411	4.7
H5a	0.188	0.034	0.109	3.7
H5b	0.255	0.076	0.200	3.7
Values for Atoms Refined with 50% Occupancy				
S11	0	0.90792(20)	0.1656(5)	3.08(15)
O11	0	0.9502(3)	0.3030(7)	6.3(3)
O12	0.9169(6)	0.9028(7)	0.0833(12)	4.3(4)
C11	0	0.8142(11)	0.2562(17)	3.1(7)
F11	0	0.7668(4)	0.1626(12)	5.1(5)
F12	0.9477(8)	0.8099(5)	0.3267(14)	8.3(6)
S21	0	0.8699(3)	0.2589(4)	4.86(23)
O22	0.9056(9)	0.8442(12)	0.2862(18)	15.4(12)
C21	0	0.8833(8)	0.0663(19)	3.8(7)
F21	0	0.8239(6)	-0.0046(11)	6.4(5)
F22	0.9444(11)	0.9239(9)	0.0313(14)	15.2(12)

<sup>a</sup> Esd's refer to the last digit printed. <sup>b</sup> B<sub>iso</sub> is the mean of the principal axes of the thermal ellipsoid.

with the formulation. The neutral ligand was prepared by deprotonation using 4 equiv of sodium hydroxide and was insoluble in water at room temperature. The Zn<sup>2+</sup> complex was prepared by reaction of the ligand triflate salt with Zn(CF<sub>3</sub>SO<sub>3</sub>)<sub>2</sub> followed by neutralization with triethylamine. This reaction yielded a single, colorless crystalline product having an elemental composition corresponding to Zn(C<sub>22</sub>H<sub>26</sub>N<sub>6</sub>)(CF<sub>3</sub>SO<sub>3</sub>)<sub>2</sub>. The spectral properties and structural elucidation of the complex follow.

**Infrared Spectra.** The infrared spectrum of py<sub>o</sub>2[18]dieneN<sub>6</sub>·4CF<sub>3</sub>SO<sub>3</sub>H exhibits a N-H stretching band at 3051 cm<sup>-1</sup> that shifts to 3275 cm<sup>-1</sup> in the spectrum of [Zn(py<sub>o</sub>2[18]dieneN<sub>6</sub>)](CF<sub>3</sub>SO<sub>3</sub>)<sub>2</sub>, indicative of coordination of the secondary amines to zinc. Coordination of the pyridine nitrogen to zinc is indicated by the shift of the high-energy pyridine band<sup>29</sup> from 1579 cm<sup>-1</sup> in the spectrum of py<sub>o</sub>2[18]dieneN<sub>6</sub>·4CF<sub>3</sub>SO<sub>3</sub>H to 1589 cm<sup>-1</sup> in the spectrum of [Zn(py<sub>o</sub>2[18]dieneN<sub>6</sub>)](CF<sub>3</sub>SO<sub>3</sub>)<sub>2</sub>. There is no band at 1350 cm<sup>-1</sup>, indicative of coordinated triflate,<sup>30</sup> found for either compound. The presence of ionic triflate is confirmed<sup>31</sup> by two bands at 1303 and 1261 cm<sup>-1</sup> in the spectrum of py<sub>o</sub>2[18]dieneN<sub>6</sub>·4CF<sub>3</sub>SO<sub>3</sub>H and at 1296 and 1244 cm<sup>-1</sup> in the spectrum of [Zn(py<sub>o</sub>2[18]dieneN<sub>6</sub>)](CF<sub>3</sub>SO<sub>3</sub>)<sub>2</sub>.

**<sup>13</sup>C-NMR Spectra.** The proton decoupled spectrum of [Zn(py<sub>o</sub>2[18]dieneN<sub>6</sub>)](CF<sub>3</sub>SO<sub>3</sub>)<sub>2</sub> in either D<sub>2</sub>O or DMSO-*d*<sub>6</sub> (Table 1) exhibits only five <sup>13</sup>C resonances. This fact indicates that the four quadrants of the macrocyclic ligand are chemically and magnetically equivalent in the complex. In order to achieve this, the macrocycle must be twisted symmetrically in a meridional mode about Zn<sup>2+</sup>, yielding a complex with D<sub>2</sub> symmetry. Isomer V (Figure 1), which has stereochemistry at the amine nitrogen sites corresponding to RRRR or SSSS chirality<sup>32</sup> when coor-

- (29) Gill, N. S.; Nuttall, R. H.; Scaife, D. E.; Sharp, D. W. A. *J. Inorg. Nucl. Chem.* **1961**, *18*, 79-87.  
 (30) Dixon, N. E.; Jackson, W. G.; Lancaster, M. J.; Lawrance, G. A.; Sargeson, A. M. *Inorg. Chem.* **1981**, *20*, 470-476.  
 (31) Dixon, N. E.; Lawrance, G. A.; Lay, P. A.; Sargeson, A. M. *Inorg. Chem.* **1984**, *23*, 2940-2947.  
 (32) Cahn, R. S.; Ingold, C. K.; Prelog, V. *Angew. Chem., Int. Ed. Engl.* **1966**, *5*, 385-415.

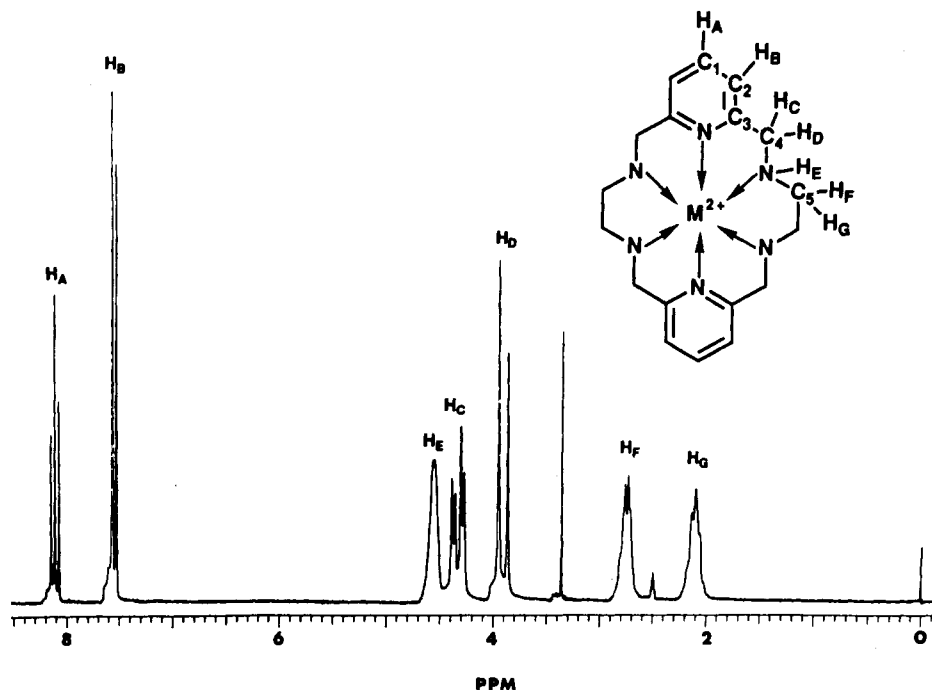


Figure 3.  $^1\text{H-NMR}$  spectrum of  $[\text{Zn}(\text{pyO}_2[18]\text{dieneN}_6)]^{2+}$  in  $\text{DMSO-}d_6$  with internal TMS.

minated, has three  $C_2$  rotational axes and is the single isomer capable of twisting to make a meridional pseudooctahedral wrap having  $D_2$  symmetry (Figure 2). Addition of excess free ligand to a  $\text{D}_2\text{O}$  solution of the complex produced a spectrum showing superposition of free and complexed ligand, indicating that ligand exchange is slow on the time scale of the NMR experiment. Additionally, there were no changes in the chemical shifts of the carbon resonances even after several months in solution, consistent with the known thermodynamic stability of  $[\text{Zn}(\text{pyO}_2[18]\text{dieneN}_6)]^{2+}$ .<sup>24</sup> Relative to those of the protonated free ligand, the  $\alpha$ -,  $\gamma$ -, and  $\beta$ -carbons of the pyridine ring in  $[\text{Zn}(\text{pyO}_2[18]\text{dieneN}_6)]^{2+}$  are slightly shifted, alternating in sign, positive for  $\alpha$  and  $\gamma$  and negative for  $\beta$ . Similar shift patterns have been reported for N-protonated pyridine.<sup>33</sup> The largest observed shifts relative to those of the free ligand are for the carbon atoms of the ethylenic linkage, which are shifted upfield by 5.2 ppm. In contrast, the methylenic carbon adjacent to pyridine is shifted downfield by 0.5 ppm.

**$^1\text{H-NMR}$  Spectra.** The spectral data for the tetraprotonated macrocyclic ligand and the  $\text{Zn}^{2+}$  complex are reported in Table 2. The assignments correspond to the labels in Figure 3, where the spectrum recorded in  $\text{DMSO-}d_6$  is shown. The pyridine protons exhibit the expected splitting patterns and chemical shifts. The tetraprotonated metal-free macrocycle has a broad resonance at 9.01 ppm assigned to  $\text{H}^+$  exchanging between the ionic triflates and the macrocyclic amines. This resonance is close to that observed for  $\text{H}^+$  in anhydrous  $\text{CF}_3\text{SO}_3\text{H}$  in  $\text{DMSO-}d_6$ .<sup>34</sup> This peak is not observed in the spectrum of  $[\text{Zn}(\text{pyO}_2[18]\text{dieneN}_6)](\text{CF}_3\text{SO}_3)_2$ . Upon complexation of the macrocycle to zinc, the amine hydrogens ( $\text{H}_E$ ) appear as a broad resonance at 4.56 ppm.  $\text{H}_C$  and  $\text{H}_D$ , resonances for which appear as a singlet in spectrum of the free ligand, are inequivalent and form the AB part of an ABX spin system,<sup>35</sup> where X is the vicinal amine hydrogen  $\text{H}_E$ . The geminal coupling is 16.8 Hz.  $\text{H}_D$  is not split by  $\text{H}_E$ , but  $\text{H}_C$  has  $^3J_{\text{H}_C-\text{H}_E}$  of 5.8 Hz. This coupling was verified by the COSY spectrum, which shows that  $\text{H}_C$  is coupled to  $\text{H}_E$  whereas  $\text{H}_D$  is not. In addition, a homonuclear decoupling

experiment where  $\text{H}_E$  was irradiated resulted in the collapse of the doublet of doublets for  $\text{H}_C$  into a single doublet and had no effect on  $\text{H}_D$ .

The spectrum of  $[\text{Zn}(\text{pyO}_2[18]\text{dieneN}_6)]^{2+}$  in  $\text{D}_2\text{O}$  (Figure 4, bottom spectrum) has splitting patterns identical to those recorded in  $\text{DMSO-}d_6$ . Surprisingly, the presence of the amine proton peak (overlapping the  $\text{H}_D$  doublet) indicates **no exchange** of NH for ND in  $\text{D}_2\text{O}$ . Repetitive scans of the spectrum over a 3-week period showed little or no exchange. Exchange of NH for ND could be induced by addition of either DCl or NaOD. After exchange, the broadened doublet splitting pattern ( $J = 16.8$  Hz) for  $\text{H}_D$  becomes sharp and the doublet of doublets pattern for  $\text{H}_C$  collapses into a single doublet ( $J = 16.8$  Hz). In order to follow the process of NH/ND exchange, the pH of  $[\text{Zn}(\text{pyO}_2[18]\text{dieneN}_6)]^{2+}$  in  $\text{D}_2\text{O}$  was adjusted to 6.8 with 0.1 M  $\text{KH}_2\text{PO}_4$  and repetitive NMR scans were taken (Figure 4). The exchange of NH for ND was observed to be complete after approximately 1 h. These results verify that NH/ND exchange does not occur in neutral solution but is both acid and base catalyzed. This behavior is indicative of a complex with unusual structural rigidity and inertness toward metal exchange in solution.

The observation that  $\text{H}_C$  is coupled to  $\text{H}_E$ , while  $\text{H}_D$  is not, can be understood in terms of the stereochemistry about the amine nitrogen atom and the ethylenic carbon atoms. The Karplus equation<sup>36</sup>

$$^3J_{\text{H-H}} = 8.5 \cos^2 \Phi - 0.28$$

can be used to predict the dihedral angle ( $\Phi$ ) from known vicinal coupling constants. The Newman projection for the complexes, viewed down the nitrogen-carbon bond (carbon adjacent to the pyridine ring), is shown in Figure 5. For a vicinal coupling constant of 5.8 Hz, as is observed in the  $\text{Zn}^{2+}$  complex, a dihedral angle of  $32.2^\circ$  between  $\text{H}_C$  and  $\text{H}_E$  is predicted. If  $\Phi_{\text{CE}}$  is  $32.2^\circ$ , then, assuming  $120^\circ$  between each substituent,  $\Phi_{\text{DE}}$  is  $87.8^\circ$ . The Karplus equation predicts that  $^3J_{\text{DE}}$  will be 0.27 Hz, which is too small to be observed. These dihedral angles are close to those determined crystallographically for the structure of  $[\text{Zn}(\text{pyO}_2[18]\text{dieneN}_6)]^{2+}$ , where  $\Phi_{\text{CE}}$  is  $31.8^\circ$  and  $\Phi_{\text{DE}}$  is  $84.8^\circ$  (*vide infra*).

(33) Pugmire, R. J.; Grant, D. M. *J. Am. Chem. Soc.* **1968**, *90*, 697-706.

(34) Dixon, N. E.; Jackson, G. A.; Lay, P. A.; Sargeson, A. M. *Inorg. Chem.* **1984**, *23*, 2940-2947.

(35) Emsley, J. W.; Feeney, J.; Sutcliffe, L. H. *High Resolution Nuclear Magnetic Spectroscopy*; Pergamon: London, 1966; Vol. 1.

(36) Karplus, M. *Chem. Phys.* **1959**, *30*, 11-15.

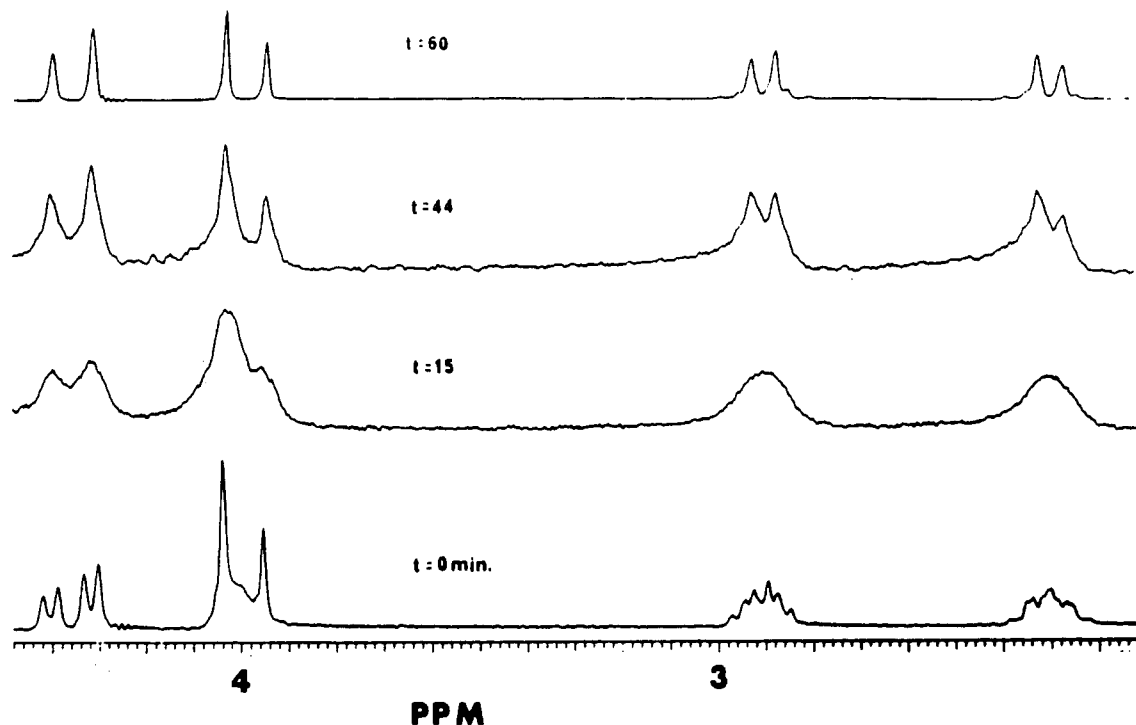


Figure 4.  $^1\text{H-NMR}$  spectra of  $[\text{Zn}(\text{pyO}_2[18]\text{dieneN}_6)]^{2+}$  in  $\text{D}_2\text{O}$  taken at time intervals after adjustment of pH to 6.8 with 0.1 M  $\text{KH}_2\text{PO}_4$ .

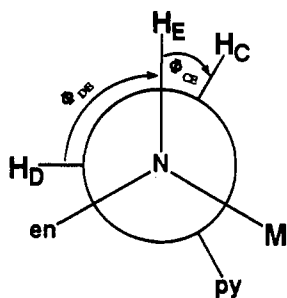


Figure 5. Newman projection along the C-N bond with  $\phi_{\text{CE}} = 30^\circ$ .

The hydrogens of the ethylenic linkage,  $\text{H}_\text{F}$  and  $\text{H}_\text{G}$ , are split into what appears at first inspection to be two complex multiplets centered at 2.75 and 2.10 ppm. The COSY spectrum shows that both of these protons are coupled to each other as well as to  $\text{H}_\text{E}$ . The addition of  $\text{DCl}$  or  $\text{NaOD}$  to  $[\text{Zn}(\text{pyO}_2[18]\text{dieneN}_6)]^{2+}$  in  $\text{D}_2\text{O}$  causes  $\text{NH/ND}$  exchange resulting in the collapse of each multiplet into a doublet ( $J = 10.6$  Hz). In a homonuclear proton-decoupling experiment on  $[\text{Zn}(\text{pyO}_2[18]\text{dieneN}_6)]^{2+}$  in  $\text{DMSO-}d_6$  in which  $\text{H}_\text{E}$  is irradiated, each of the multiplets also appears as a doublet ( $J = 10.6$  Hz).

Spin simulation of the multiplets using the Laocoon program<sup>37</sup> and an AA'BB'XX' spin system with coupling constants calculated by the Karplus equation using the dihedral angles derived from the crystal structure reproduced the experimental spectrum (Figure 6). Comparison with the splitting patterns for other diamagnetic macrocyclic complexes containing ethylenic linkages reveals that, to our knowledge, this is the first report of the detailed assignment and simulation of an AA'BB'XX' pattern for this type of linkage in a macrocyclic complex. This is an indication of the unusual nature of  $[\text{Zn}(\text{pyO}_2[18]\text{dieneN}_6)]^{2+}$  related to its extreme stereochemical and regiochemical rigidity.

**UV Spectrum.** In aqueous solution,  $[\text{Zn}(\text{pyO}_2[18]\text{dieneN}_6)]^{2+}$  has a band at 266 nm and a shoulder at approximately 220 nm. The  $\pi$  to  $\pi^*$  transition in the UV spectrum of pyridine occurs at 256 nm.<sup>38</sup> The  $\pi$  to  $\pi^*$  transition in 2,6-dimethylpyridine occurs at 270 nm.<sup>37</sup> The transition at 266 nm for  $[\text{Zn}(\text{pyO}_2[18]\text{dieneN}_6)]^{2+}$

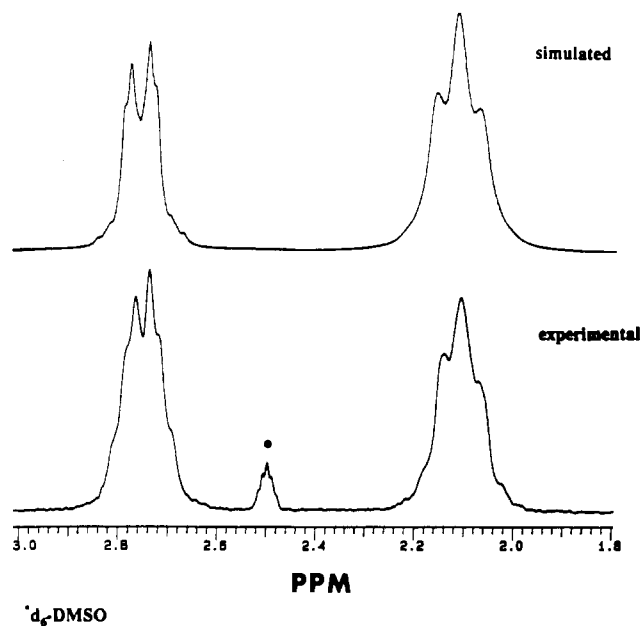


Figure 6. Simulated spectrum: An AA'BB'XX' spin system with  $^2J_{\text{AB}} = ^2J_{\text{A'B'}} = -10$  Hz,  $^3J_{\text{AB'}} = ^3J_{\text{A'B}} = 1.0$  Hz,  $^3J_{\text{AA'}} = 2.8$  Hz,  $^3J_{\text{BB'}} = 9.1$  Hz,  $^3J_{\text{AX}} = ^3J_{\text{A'X'}} = 2.8$  Hz,  $^3J_{\text{BX}} = ^3J_{\text{B'X'}} = 9$  Hz,  $^4J_{\text{AX}} = ^4J_{\text{A'X'}} = ^4J_{\text{BX}} = ^4J_{\text{B'X'}} = ^5J_{\text{XX'}} = 0$  Hz, and a bandwidth of 1.5. Experimental spectrum: The observed spectrum of  $\text{H}_\text{F}$  and  $\text{H}_\text{G}$  in  $[\text{Zn}(\text{pyO}_2[18]\text{dieneN}_6)]^{2+}$ .

$(\text{CF}_3\text{SO}_3)_2$  is thus assigned to the  $\pi$  to  $\pi^*$  transition of pyridine. The absorption spectrum closely resembles that of pyridine in protic solvents. The weaker n to  $\pi^*$  shoulder is not visible in the spectrum and therefore must be buried under the more intense  $\pi$  to  $\pi^*$  transition. The interaction of the pyridine nitrogen lone pair with a metal cation has little effect on the energy of the  $\pi$  to  $\pi^*$  transition.<sup>39</sup> Thus, there is no shift in the energy of the  $\pi$  to  $\pi^*$  transition of pyridine in  $[\text{Zn}(\text{pyO}_2[18]\text{dieneN}_6)](\text{CF}_3\text{SO}_3)_2$  relative to  $\text{pyO}_2[18]\text{dieneN}_6 \cdot 4\text{CF}_3\text{SO}_3\text{H}$ .

(38) Andon, R. L.; Cox, J. D.; Herrington, E. F. G. *Trans. Faraday Soc.* 1954, 50, 918-927.

(39) Dyer, R. B.; Palmer, R. A.; Ghirardelli, R. G.; Bradshaw, J. S.; Jones, B. A. *J. Am. Chem. Soc.* 1987, 109, 4780-4786.

(37) Bothner-by, A. A.; Castellano, S. *J. Chem. Phys.* 1964, 41, 3863-3869.

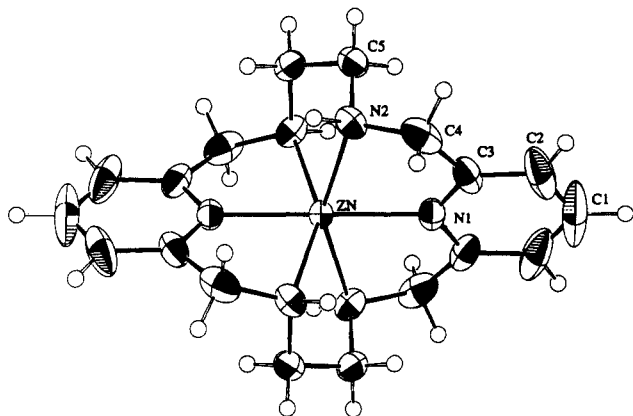


Figure 7. ORTEP diagram of  $[\text{Zn}(\text{pyO}_2[18]\text{dieneN}_6)]^{2+}$ .

**Optical Resolution of  $[\text{Zn}(\text{pyO}_2[18]\text{dieneN}_6)](\text{CF}_3\text{SO}_3)$ .** Racemic  $[\text{Zn}(\text{pyO}_2[18]\text{dieneN}_6)]^{2+}$  was resolved into diastereomers using barium (+)-tartrate. (+)- $[\text{Zn}(\text{pyO}_2[18]\text{dieneN}_6)]$  (+)-tartrate is only slightly soluble in water and precipitates as colorless crystals, leaving the other diastereomer in solution. Evaporation of the mother liquor results in the isolation of (-)- $[\text{Zn}(\text{pyO}_2[18]\text{dieneN}_6)]$ -(-)-tartrate. To remove the optically active anion, the two diastereomers were converted to their triflate salts, (+)- $[\text{Zn}(\text{pyO}_2[18]\text{dieneN}_6)](\text{CF}_3\text{SO}_3)_2$  ( $\alpha_{589} = +0.0030 \pm 0.0005^\circ$  for a 0.1% aqueous solution) and (-)- $[\text{Zn}(\text{pyO}_2[18]\text{dieneN}_6)](\text{CF}_3\text{SO}_3)_2$  ( $\alpha_{589} = -0.0025 \pm 0.0005^\circ$  for a 0.1% aqueous solution). The  $^1\text{H}$ - and  $^{13}\text{C}$ -NMR spectra of the enantiomers in  $\text{DMSO}-d_6$  were identical to those of racemic  $[\text{Zn}(\text{pyO}_2[18]\text{dieneN}_6)]^{2+}$ . No racemization of (-)- $[\text{Zn}(\text{pyO}_2[18]\text{dieneN}_6)](\text{CF}_3\text{SO}_3)_2$  was observed after 6 months in neutral, aqueous solution at room temperature. The CD spectra of (+)- $[\text{Zn}(\text{pyO}_2[18]\text{dieneN}_6)](\text{CF}_3\text{SO}_3)_2$  and (-)- $[\text{Zn}(\text{pyO}_2[18]\text{dieneN}_6)](\text{CF}_3\text{SO}_3)_2$  in aqueous solution give a positive and corresponding negative Cotton effect of approximately 19 mdeg for a 0.1% solution at 262 nm in the CD spectra (see Experimental Section). The spectra were unchanged after 20 h. The appearance of CD bands indicates that, upon coordination to  $\text{Zn}^{2+}$ , a conformationally rigid macrocyclic complex is formed that persists in solution, allowing the separation and isolation of  $\Delta$  and  $\Lambda$  enantiomeric forms. Racemic  $[\text{Zn}(\text{pyO}_2[18]\text{dieneN}_6)](\text{CF}_3\text{SO}_3)_2$  does not give a CD spectrum. The NMR results described above indicate that the complexes do not undergo the metal ion dissociation or interconversion of nitrogen stereochemistry that would be required to interconvert the enantiomers. These data further confirm the helical structure and the exceptional kinetic stability of the complexes in aqueous solution.

**X-ray Crystal Structure of  $[\text{Zn}(\text{pyO}_2[18]\text{dieneN}_6)](\text{CF}_3\text{SO}_3)_2$ .** In order to better understand the structural features of  $\text{pyO}_2[18]\text{dieneN}_6$  when coordinated to  $\text{Zn}^{2+}$ , a crystallographic analysis was performed. Recrystallization of  $[\text{Zn}(\text{pyO}_2[18]\text{dieneN}_6)](\text{CF}_3\text{SO}_3)_2$  from water gave colorless orthorhombic crystals containing no solvent. The crystallographic summary is given in Table 3. The ORTEP diagram of  $[\text{Zn}(\text{pyO}_2[18]\text{dieneN}_6)]^{2+}$  is shown in Figure 7, and a stereoview is shown in Figure 8. The relative positions of the hydrogen atoms on the amines correspond to ligand isomer V (Figure 1). The macrocycle is twisted, with the two pyridine rings oriented  $104.5^\circ$  relative to each other. The twisting of the macrocycle gives rise to two meridional linkages, each incorporating one pyridine nitrogen and the two adjacent aliphatic amines. The coordination sphere is distorted in that two *trans* aliphatic amines of one meridional span are displaced  $0.567 \text{ \AA}$  above the equatorial plane while the other two *trans* aliphatic amines are an equal distance below the plane. A similar distortion is observed for various  $[\text{M}(18)\text{aneN}_2\text{S}_4]^{2+}$  complexes.<sup>40</sup>

Selected bond distances and angles are listed in Table 4. The two  $\text{Zn}-\text{N}_{\text{py}}$  distances are  $2.112 (5) \text{ \AA}$ , and the four  $\text{Zn}-\text{N}_{\text{am}}$  distances are equivalent by symmetry at  $2.210(4) \text{ \AA}$  each. The longer  $\text{Zn}^{2+}-\text{N}_{\text{am}}$  bond distances compared to the  $\text{Zn}^{2+}-\text{N}_{\text{py}}$  bond distances are as expected.<sup>41</sup> The  $\text{Zn}^{2+}-\text{N}_{\text{am}}$  bond distances within the macrocycle are comparable to octahedral nonmacrocyclic  $\text{Zn}^{2+}-\text{N}_{\text{am}}$  bond distances ( $\text{\AA}$ ), as in  $\text{Zn}(\text{en})_3\text{Cl}_2 \cdot 2\text{H}_2\text{O}$  ( $2.209(9)$ ,  $2.23(1)$ ,  $2.209(9)$ ),<sup>42</sup>  $\text{Zn}(\text{en})_3\text{F}_2 \cdot 2\text{H}_2\text{O}$  ( $2.176(4)$ ,  $2.211(4)$ ,  $2.187(4)$ ),<sup>43</sup>  $\text{Zn}(\text{en})_3\text{Ni}(\text{CN})_4 \cdot \text{H}_2\text{O}$  ( $2.213(11)$ ,  $2.250(13)$ ,  $2.257(13)$ ,  $2.200(13)$ ,  $2.216(12)$ ,  $2.204(12)$ ), and  $\text{Zn}(\text{en})_3\text{Ni}(\text{CN})_4$  ( $2.215(6)$ ,  $2.214(7)$ ,  $2.229(7)$ ,  $2.242(7)$ ,  $2.200(6)$ ,  $2.232(6)$ ).<sup>44</sup> Comparison of the  $\text{Zn}^{2+}-\text{N}_{\text{py}}$  bond distances to those of other six-coordinate zinc complexes with pyridine-containing macrocycles is not possible since none were found in the literature. However, the structure of the cobalt complex of tetra-*N*-methyl-substituted  $\text{pyO}_2[18]\text{dieneN}_6$ ,  $[\text{Co}(\text{Me}_4\text{pyO}_2[18]\text{dieneN}_6)]^{2+}$ , was determined by Newkome et al.<sup>45</sup> In this case, the macrocycle is twisted similarly to the macrocycle in  $[\text{Zn}(\text{pyO}_2[18]\text{dieneN}_6)]^{2+}$ . The  $\text{Co}^{2+}-\text{N}_{\text{py}}$  bond distances are  $0.18 \text{ \AA}$  shorter than the  $\text{Co}^{2+}-\text{N}_{\text{am}}$  bond distances. The two pyridine rings are twisted  $101^\circ$  relative to each other. Similarly, the distortion of the aliphatic amine nitrogens from planarity is qualitatively the same as in  $[\text{Zn}(\text{pyO}_2[18]\text{dieneN}_6)]^{2+}$ .

The twist of  $\text{pyO}_2[18]\text{dieneN}_6$  about  $\text{Zn}^{2+}$  gives rise to  $\Delta\delta\delta$  and  $\Delta\lambda\lambda$  isomers.<sup>46</sup> The C-C bond distances of  $1.509(9) \text{ \AA}$  for the five-membered chelate rings within the macrocycle are in the reported range of  $1.41\text{--}1.57 \text{ \AA}$  for ethylenediamine complexes.<sup>41</sup> The conformation of the diaminoethane chelate rings within the macrocycle is gauche. This conformation has been defined by several criteria in ethylenediamine complexes.<sup>47,48</sup> The first of these is that the dihedral angle between the plane defined by one nitrogen atom and the two carbons of the ethylenediamine ring and the plane defined by the two carbons of the ethylenediamine ring and the other nitrogen atom should be approximately  $50^\circ$ . This dihedral angle is  $63.5^\circ$  in  $[\text{Zn}(\text{pyO}_2[18]\text{dieneN}_6)]^{2+}$ . A second criterion is that the angle between the plane defined by the metal ion and the two nitrogen atoms and the plane defined by the metal ion and the two carbon atoms should be greater than  $0^\circ$  (approximately  $25^\circ$ ), since if it were  $0^\circ$ , this would be the eclipsed configuration. This angle is  $33^\circ$  in  $[\text{Zn}(\text{pyO}_2[18]\text{dieneN}_6)]^{2+}$ . The final criterion is that the deviation of the two carbon atoms from the plane of the metal ion and the two nitrogen atoms should be symmetric above and below. The  $D_2$  symmetry of the complex requires this last criterion.

For  $\text{M}(\text{en})_2$  complexes there are six possible conformational isomers:<sup>46</sup>  $\Delta\lambda\lambda$ ,  $\Delta\delta\delta$ ,  $\Delta\delta\lambda$ ,  $\Delta\lambda\lambda$ ,  $\Delta\delta\delta$ ,  $\Delta\delta\lambda$ . Because of the symmetry of  $[\text{Zn}(\text{pyO}_2[18]\text{dieneN}_6)]^{2+}$ , only the isomers  $\Delta\lambda\lambda$ ,  $\Delta\delta\delta$ ,  $\Delta\lambda\lambda$ ,  $\Delta\delta\delta$  are possible. Since the space group  $I\text{m}cb$  is centrosymmetric, the crystals contain a racemic mixture of one of the two pairs of enantiomorphs, either ( $\Delta\lambda\lambda$ ,  $\Delta\delta\delta$ ) or ( $\Delta\delta\delta$ ,  $\Delta\lambda\lambda$ ). Examination of Figure 7 shows that the latter pair of enantiomorphs is present in the crystal structure. This is consistent with the presence of only one set in the experimental optical resolution of the enantiomers.

The methylenic carbons of pyridine form the termini of two chains of atoms, including the ethylenediamine moieties, that

- (41) Melson, G. A., Ed. *Coordination Chemistry of Macrocyclic Compounds*; Plenum: New York, 1979, p 268.  
 (42) Muralikrishna, C.; Mahadevan, C.; Sastry, S.; Seshasayee, M.; Subramanian, S. *Acta Crystallogr., Sect. C* **1983**, *39*, 1630.  
 (43) Emsley, J.; Arif, M.; Bates, P. A.; Hurthouse, M. B. *Inorg. Chim. Acta* **1989**, *165*, 191-195.  
 (44) Cernak, J.; Chonic, J.; Dunaj-Jurco, M.; Kappenstein, C. *Inorg. Chim. Acta* **1984**, *85*, 219-226.  
 (45) Newkome, G. R.; Majestic, V. K.; Fronczek, F. R. *Inorg. Chim. Acta* **1983**, *77*, L47-L49.  
 (46) Leigh, G. J., Ed. *Nomenclature of Inorganic Chemistry*; Blackwell Scientific: Oxford, U.K., 1991; pp 182-185.  
 (47) Raymond, K. N.; Cornfield, P. W. R.; Ibers, J. A. *Inorg. Chem.* **1968**, *7*, 842-844.  
 (48) Cullen, D. L.; Lingafelter, E. C. *Inorg. Chem.* **1970**, *9*, 1858-1864.

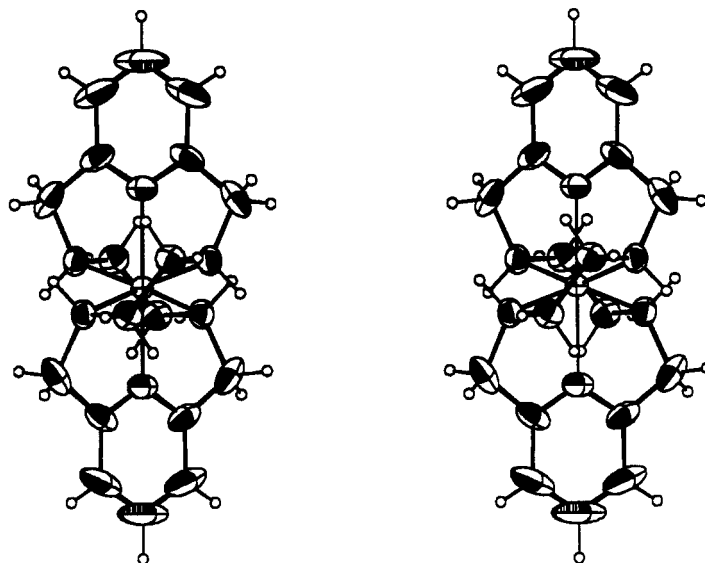


Figure 8. Stereoview of  $[\text{Zn}(\text{pyO}_2[18]\text{dieneN}_6)]^{2+}$ .

form a double helix about zinc connecting the 2- and 6-positions of the *trans* pyridine groups. The helical conformation is achieved through rotation about single bonds, as seen in the dihedral angles of 31.8 and 85.4° between H–C–N<sub>am</sub>–H for the two geminal hydrogen atoms on C4. The helical linkages must be held rigidly by coordination since the <sup>1</sup>H NMR patterns give exquisite evidence for absence of fluctional motion or averaging of coupling constants. The twisting of the macrocycle to accommodate Zn<sup>2+</sup> also is achieved by rotation about the bonds between the amine nitrogens and the carbons of the ethylenic linkages. This rotation pulls the N<sub>am</sub> atoms in to accommodate the Zn–N distance and decreases the dihedral angle N–C–C–N of the ethylenic linkage. The δ (λ) conformation of the ethylenic linkage also is rigidly retained in solution since an AA'BB'XX' spin system is observed. For equal populations of the δ and λ conformations, an A<sub>4</sub>X<sub>2</sub> spin system would be observed.

**Conclusions.** pyO<sub>2</sub>[18]dieneN<sub>6</sub> shows a remarkable capability for “twisting” in a helical fashion in order to wrap about a small metal ion. Only one of the five possible N–H isomers (V) can perform this twist in D<sub>2</sub> symmetry. Isomerism in the complex arises from two sources: the stereochemistries at nitrogen and the direction in which the helical linkages twist around Zn<sup>2+</sup>. Although four possible twisted forms can be derived from V plus twist, only two are observed, a consequence of the fact that each

enantiomer of V can twist in only one direction. Thus, the crystal structure contains a single enantiomeric pair of isomer V coordinated, each twisted in the opposite sense. Optical resolution of this novel  $[\text{Zn}(\text{pyO}_2[18]\text{dieneN}_6)]^{2+}$  complex was achieved due to its extreme stability and kinetic inertness toward N–H exchange and metal exchange in neutral aqueous solution. This kinetic inertness may be related to the fact that six metal–nitrogen bonds must be broken approximately simultaneously in order to “untwist” the macrocycle to release the metal ion. Also, four nitrogen atoms must undergo inversion to convert from one enantiomer to the other. Although twisted isomer V is the preferred conformation of the ligand when coordinated to small metal ions, it will be of interest to determine whether these regio- and stereospecificities persist when the ligand is coordinated to larger metal ions.

**Acknowledgment.** The authors thank Dr. Peter White at UNC—Chapel Hill for assistance with the crystal structure. This research was supported by grants from the National Institutes of Health (GM-41919) and the National Science Foundation (CHE-9308988).

**Supplementary Material Available:** Listings of anisotropic thermal parameters, bond distances, bond angles, and torsion angles (6 pages). Ordering information is given on any current masthead page.